Cytometry 23:205–217 (1996)

Improved Four-Color Flow Cytometry Method Using Fluo-3 and Triple Immunofluorescence for Analysis of Intracellular Calcium Ion ($[Ca^{2+}]_i$) Fluxes Among Mouse Lymph Node B- and T-Lymphocyte Subsets

Roland Greimers, Mohamed Trebak, Michel Moutschen, Nathalie Jacobs, and Jacques Boniver

Laboratory of Pathological and Cytological Anatomy, University Hospital of Liège, Liège, Belgium

Received for publication April 7, 1995; accepted November 14, 1995

A visible-light, dual-laser, flow cytometric method was developed for the simultaneous analysis of intracellular ionized calcium concentration ($[Ca^{2+}]_i$) and three cell-surface markers (CD4, CD8, and Thy-1.2 antigens) by using the calcium probe fluo-3 and using R-phycoerythrin (PE), peridinin chlorophyll-α protein (PerCP), and allophycocyanin (APC) conjugated monoclonal antibodies (MoAbs). This improved method was used in the analysis of $[Ca^{2+}]_i$ mobilization upon in vitro stimulation with mitogenic lectins [phytohaemagglutinin (PHA) or concanavalin A (ConA)], anti-CD3 MoAbs, or A23187 calcium ionophore in the heterogeneous lymph node cell populations from healthy C57BL/Ka mice. The present results show that the calcium responses were heterogeneous and dependent on the cellular immunophenotype, not only on lectins or anti-CD3 MoAbs stimulation, but also on the receptor-independent A23187 ionophore stimulation. An in situ fluo-3 calibration method (using A23187 and metabolic poisons in Ca^{2+}/EGTA buffers with known free calcium concentrations) indicated a resting $[Ca^{2+}]_i$ in lymphocytes of 103 ± 23 nM (mean ± S.D.) but with significant differences between the $[Ca^{2+}]_i$ in B cells and in all of the T-cell subsets ($CD4^+Thy\text{-}1^+$, $CD4^+Thy\text{-}1^-$, and $CD8^+$ T cells). Both the B cells and the T-cell subsets showed an increase of fluo-3 fluorescence upon in vitro stimulation with ConA or PHA, but the calcium mobilization following lectin stimulation was time delayed in all T-cell subsets. Only the T cells, including the $CD4^+Thy\text{-}1^-$ subset, responded to anti-CD3 MoAbs. The percentage of responding cells upon stimulation with ConA was higher in T cells than in B cells. By contrast, PHA gave a higher response in B cells. After stimulation with different mitogens, $[Ca^{2+}]_i$ increased in both $CD4^+$ and $CD8^+$ T-cell subsets. However, the percentage of responding cells was far higher in the $CD4^+Thy\text{-}1^+$ subset than in the $CD4^+Thy\text{-}1^-$ or the $CD8^+$ T-cell subsets. The stimulation with A23187 ionophore induced a higher calcium response in B cells than in T cells. Interestingly, it also induced greater Ca^{2+} mobilization in $CD4^+$ than in $CD8^+$ T cells. These results demonstrate the potential use of fluo-3 simultaneously with three fluorescein (FITC)-compatible fluorochromes. This technique may be useful for investigating the role of the $CD4^+Thy\text{-}1^-$ T cells, a rare subset that is abnormally expanded in a murine acquired immunodeficiency syndrome (murine AIDS). © 1996 Wiley-Liss, Inc.

Key terms: Calcium fluxes, mouse lymph node lymphocytes, fluo-3 in situ calibration, nigericin, CCCP, phycoerythrin, peridinin chlorophyll-α tandem (PerCP), allophycocyanin, four-color flow cytometry

Cytoplasmic free calcium ($[Ca^{2+}]_i$) plays a central role in the transduction of external stimuli in many cell types (45), including T lymphocytes (7,8,11,18,19,33). With the introduction of calcium-sensitive fluorochromes, measurement of intracellular calcium has become a fascinating new tool for studying the early events of cell activation in intact cells either by image analysis (8,26, 40,50) or by flow cytometry (23,42,44,50). However, the first $[Ca^{2+}]_i$ indicators, such as quin-2, fura-2, or indo-1 (12,43,52,53), were not excitable by visible light, and the requirement for a UV-laser posed a considerable limitation in most laboratories. Fortunately, the spectral properties of fluo-3 (25,34), which is the newest of these

N.J. is supported by a grant from the Leon Fredericq Foundation. M.T. is supported by a grant from the Centre Anticancéreux près l'Université de Liège (CAC).

The first two authors contributed equally to this work.

Address reprint requests to R. Greimers, Laboratory of Pathologic Anatomy, University Hospital of Liège B35, B4000 Liège, Belgium.

Ca^{2+} dyes, allows the analysis of $[Ca^{2+}]_i$ by most flow cytometers that are equipped with the usual 488-nm-line, argon-ion laser excitation source and fluorescein (FITC) filter bandwidth (46,54). In addition, the large enhancement of green fluorescence intensity on Ca^{2+} binding could be measured in two-color flow cytometry with the simultaneous analysis of cell surface immunolabelling performed either with R-phycoerythrin (PE; orange fluorescence; 31,47), or with PE-Texas red tandem (Red-613; red fluorescence; 6), or with peridinin chlorophyll-α protein complex (PerCP; far red fluorescence; 13) conjugated monoclonal antibodies (MoAbs). The availability of allophycocyanin (APC)-conjugated MoAbs theoretically offers the opportunity to perform five-color flow cytometry by combination with fluo-3, PE, PE-Texas red tandem, and PerCP. However, APC is only excited by red light, and a second laser must be focused on the stream to stimulate the far red fluorescence signal of this dye. Therefore, the means to perform multicolor experiments in calcium studies among complex immunophenotypic cell subsets is now feasible by using fluo-3 in conjunction with more than one fluorescent MoAb and a visible excitation laser light, but this has not been described previously.

This paper describes an original method that allows the simultaneous flow cytometry of fluo-3-$[Ca^{2+}]$ in conjunction with PE-, and PerCP-, and APC-conjugated MoAbs by using lymph node (LN) cells from normal mice. The method is useful for the analysis of $[Ca^{2+}]_i$ in a heterogeneous LN cell population, including the B cells, the $CD8^+$ cells, and the $CD4^+Thy\text{-}1^+$ T cells. We also focused our attention on the peculiar $CD4^+Thy\text{-}1^-$ T-cell subset, which has been described in normal spleen, LNs, lamina propria, peritoneum, and in Peyer's patches (14). These $CD4^+Thy\text{-}1^-$ cells accumulate in the peripheral lymphoid tissues of mice, which develop the retroviral-induced immunodeficiency syndrome (murine AIDS or MAIDS), a pathological model that is associated with serious alterations of signal-transduction pathways (3,4,9, 16,17,21,29,31,35,37,38). This phenotypic abnormality is interesting, because Thy-1 is associated with $p59^{fyn}$, a protein tyrosine kinase (PTK) that is involved in signal transduction in T cells (27,51). We applied our visible-light flow cytometric method to detect cytoplasmic free calcium in healthy mice by using time-course analysis in conjunction with three MoAbs directed against CD4, CD8, and Thy-1 antigens.

MATERIALS AND METHODS

Mice and Cell Suspension

One-month-old male C57Bl/Ka (H-2b) mice that were bred in our facility were sacrificed by CO_2 asphyxiation. Inguinal and axillary LN were removed, and single-cell suspensions were prepared with a fitting glass homogenizer (tolerance of pestle, 15–25 μm), passed through a nylon cell strainer, washed three times with phosphate buffered saline (PBS), and counted on a Thomas hemacytometer, as described previously (38).

Antibodies and Second-Step Reagent

The following MoAbs were used: PE-conjugated anti-CD4/L3T4 (CD4-PE; YTS.191.1), APC-conjugated anti-Thy-1.2/CD90 (Thy-1-APC; 5a-8; Caltag Laboratories, ITK Diagnostics, The Netherlands), and biotinylated anti-CD8/Lyt-2 (53-6.7; Pharmingen, ITK Diagnostics) revealed with PerCP-labelled streptavidin (Becton Dickinson, Erembodegem, Belgium; CD8-PerCP). Biotinylated anti-CD8/Lyt-2 (53-6.7; Pharmingen) revealed with PE-labelled streptavidin (CD8-PE; Becton Dickinson) and PE-conjugated anti-CD45R/B220 (RA3-6B2; B220-PE; Pharmingen) were also used for control experiments.

Preparation of Fluo-3-Loaded Cells

The cells were washed three times in Hanks buffered saline solution (HBSS) containing 1% heat-inactivated fetal calf serum (FCS); then, they were suspended in RPMI 1640 supplemented with 10% of FCS, 2 mM L-glutamine, 30 U/ml penicillin, 20 μg/ml streptomycin, 5×10^{-5} M β-mercaptoethanol, 1 mM sodium pyruvate (Techgen, Zellick, Belgium), and 1% nonessential amino acids (043-01140; Life Technologies-Gibco, Gent, Belgium). Fluo-3 was loaded into the cells as described (54), with minor modifications. A 2 mM stock solution of fluo-3-penta-acetoxymethylester (fluo-3/AM; Molecular Probes, Eugene, OR) was made with dry anhydrous dimethylsulfoxide (DMSO). A 20% w/v stock solution of Pluronic F-127 (Molecular Probes), a nonionic surfactant polyol, was made separately in DMSO. The cells (10^7 cells/ml) were first incubated in HBSS alone (without FCS) containing fluo-3/AM at a final concentration of 2 μM and 3 μl/ml of the Pluronic F-127 stock solution for 20 min at room temperature. The cells were then diluted 1/5 (2×10^6 cells/ml) with HBSS containing 1% FCS, and then they were incubated again for 40 min in a 37.5°C ± 0.1°C water bath. To obtain accurate calcium kinetics, it was crucial to maintain this temperature slightly above 37°C throughout the fluo-3 loading procedure.

Triple Immunostaining of Fluo-3-Loaded Cells

Fluo-3-loaded cells were washed three times in HBSS containing 1% FCS. After the last wash, the supernatant fluid was discarded, and the cells were resuspended in a mixture containing the Thy-1-APC, CD4-PE, and biotinylated CD8 MoAbs previously diluted in PBS as indicated by the manufacturers. A first incubation was performed for 20 min at 4°C. The second reagent streptavidin-PerCP was then added to reveal the biotinylated MoAb (CD8) and incubated as described above. The cells were then washed twice and diluted to 10^6 cells/ml with 10 mM 4-(2-hydroxyethyl)piperazin-1-ethanesulfonic acid (HEPES)-buffered salt containing NaCl 137 mM, KCl 5 mM, Na_2HPO4 1 mM, glucose 5 mM, $CaCl_2$ 1 mM, $MgCl_2$ 0.5 mM, BSA 1 g/liter, and HEPES 10 mM, pH 7.4. The cell suspensions were then placed in a water bath at 37.5°C for 15 min before flow cytometry.

Flow Cytometry

Analyses were performed by using a FACStar$^+$ flow cell sorter with the LYSYS II software (Becton Dickinson). A blue excitation at 488 nm (25 mW of power light) from an argon-ion laser (air-to-water-cooled model Spinnaker 1161; Spectra Physics, Mountain View, CA) was used for three-color analysis of fluo-3 green, PE orange, and PerCP red fluorescences. The forward- and right-angle light scatters (FSC and SSC, respectively) were used to gate the cells. Green fluorescence emission of fluo-3 was detected at 530 nm (DF 530/30 dichroic bandpass filter), PE fluorescence was measured at 575 nm (DF 575/26), and PerCP was measured at 670 nm (DF 675/20). Cross over of fluo-3 fluorescence into the PE detection window and of PE fluorescence into the PerCP detection window was electronically compensated by analog subtraction at the preamplifier stage. For four-color analysis of intracellular fluo-3-$[Ca^{2+}]_i$ and surface-labelled PE, PerCP, and APC MoAbs, the conditions were the same as above, but a spatially separated beam of a second laser (water-cooled model 164-01 krypton ion laser; Spectra-Physics) was used for excitation of APC at 647 nm (150 mW of light power). The krypton laser beam was focused onto the stream about 175 μm below the argon beam focus intersection. Consequently, the APC fluorescence signal was time delayed and was detected 20 μs after the detection of the other fluorescence signals. A half mirror and an iris aperture were adjusted in front of the APC-dedicated photomultiplier tube to achieve the separation of the fluorescences excited by the two lasers. The red fluorescence emission of APC was detected at 670 nm (DF 670/14). The flow cytometer input tubing was carefully washed with DMSO and ethanol to remove residual material before proceeding to the next sample.

Analysis of cells labelled with CD8-PerCP and/or with Thy-1-APC MoAbs demonstrated that the red PerCP fluorescence emission did not interfere with the red APC fluorescence emission, and vice versa. Additional controls for the immunofluorescence were also used. 1) CD8-PE-labelled LN cells were used for positive detection of CD8$^+$ T cells as a control for subsequent optimization of the CD8-PerCP fluorescence. 2) Dual-color flow cytometry of Thy-1-APC- and CD4-PE-labelled LN cells from mice with murine AIDS induced as described (38) was performed for accurate gating of the CD4$^+$Thy-1$^-$ cells that create a visible subset on flow cytometric dot plots, because they are abnormally expanded in this disease (4,17,38). This separation between CD4$^+$Thy-1$^+$ and CD4$^+$Thy-1$^-$ corresponded with the position of the end of the CD4$^-$Thy-1$^-$ population of healthy mice (38).

FSC and SSC and fluo-3 fluorescence were displayed on a linear scale, whereas PE, PerCP, and APC fluorescences were displayed on a four-decade logarithmic scale with a histogram resolution of 256 channels to conserve memory. The "time" parameter was activated on a scale of 512 s (500 ms/channel). The cells were analyzed at 37.5°C at typical rates of 400–600 s. The seven parameters (FSC, SSC, four-colors, and time) were stored for each measured cell in a sequential data file ("list mode"). To avoid saturation of the computer memory due to the considerable amount of data per sample, measurements were registered directly on the hard disk without transitional storing in the RAM-memory. Final data files were transferred to a 650 MB, rewritable, magnetooptical disk (EDM-1DAOs; Sony, Tokyo, Japan) inserted in a dedicated removable cartridge system (Bering 5600 OptiPac; Ocean Microsystems, Inc., Campbell, CA).

Stimulation of Lymphocytes With A23187, Mitogenic Lectins, or Anti-CD3 MoAb

At indicated times after base-line unstimulated measurements, a stimulus was added to the sample running on the flow cytometer. The cell flow was briefly (<10 s) halted at the time of mitogen addition, creating a visible gap in the data set. A23187, an antibiotic calcium ion ionophore, was used at 10 μM (Molecular Probes; stock solution in liquid nitrogen; 10 mM A23187 in DMSO). PHA was used at 10 μg/ml (PHA M; Difco, Detroit, MI; stock solution at −20°C; 1 mg/ml PHA in distilled water). ConA was used at 12.5 μg/ml (Boehringer Mannheim, Federal Republic of Germany; stock solution at −20°C; 5 mg/ml ConA in distilled water). A mitogenic murine anti-CD3 MoAb that was purified in our laboratory from hamster hybridoma 145-2C11 supernatant (30) was used at 5 μg/ml.

Calibration of the Fluo-3 Fluorescence Signal

The determination of intracellular calcium concentration in resting cell subsets identified by three-color immunolabelling was made by using a standard curve that was based on the direct calibration of fluo-3 fluorescence intensity with solutions of known calcium concentration made from mixtures of calcium salt and ethylene glycol bis(2-aminoethyl)ether N, N, N′, N′-tetraacetic acid (EGTA). The intact cells were permeabilized with calcium ionophore and metabolic poisons according to Chused et al. (5) with minor modifications. For this procedure, gradients of protons, membrane potential, and ion transport across cell and mitochondrial membranes were collapsed by nigericin, a K^+ and H^+ ionophore that clamps the pH gradient to zero; carbonyl cyanide m-chlorophenylhydrazone (CCCP), an uncoupler of mitochondrial oxidative phosphorylation that diminishes ATP production and disables ion pumping across cytoplasmic, mitochondrial, and endoplasmic reticulum membranes; and A23187, an antibiotic calcium ionophore that induces Ca^{2+}-H^+ exchange. Consequently, it was shown that intracellular $[Ca^{2+}]_i$ is made equal to the known extracellular free calcium concentration ($[Ca^{2+}]_o$) (5). The following method was then used.

Fluo-3-loaded cells were triple immunolabelled with CD4-PE, CD8-PerCP, and Thy-1.2-APC MoAbs, as described above. The cells were washed and resuspended in 120 mM KCl, 20 mM HEPES, pH 7.2, 1 mM MgSO4, 20 mM NaN3, and 10 mM 2-deoxyglucose without bicarbonate. Aliquots of cells were transferred to a series of 11

Ca^{2+}/EGTA buffers with 0–10 mM EGTA and free Ca^{2+} concentrations ranging from 0 to 39.8 μM containing 100 mM KCl, 10 mM MOPS, pH 7.2 (C-3009 calcium calibration buffer kits II; Molecular Probes Europe, Leiden, The Netherlands). These buffers were prepared according to a "pH-metric" method that has been described previously (52). The following reagents were added: 1) 0.5 μg/ml nigericin (previously dissolved in ethanol; Sigma-Aldrich, Bornem, Belgium); 2) 2 μM CCCP (previously dissolved in acetone; Sigma-Aldrich); and 3) 10 μM A23187 ionophore (previously dissolved in DMSO; Molecular Probes). Cells were incubated at 37.5°C for at least 2 h before flow cytometry. This time was long enough to obtain a stable fluo-3 fluorescence signal, which was then recorded on linear histograms (1,024 channels for best accuracy) for each cell subset identified by triple immunostaining (5,000–10,000 cells/subset). The fluo-3 mean channel fluorescence was calculated and reported as a function of free calcium concentration of the 11 Ca^{2+}/EGTA buffers (Fig. 4; 5,36,52). The calibration was carried out at the end of every experiment.

Statistical Analysis

A one-way analysis of variance (ANOVA) followed by Newman-Keuls two-tailed tests were performed by using the Instat® Mac 2.01 software (GraphPad Software, San Diego, CA).

RESULTS AND DISCUSSION

Four-Color Analysis of $[Ca^{2+}]_i$ With Fluo-3 and Triple Immunofluorescences

The presently described method is based on a seven-parameter (FSC, SSC, four colors, and time) analysis of heterogeneous cell populations using fluo-3, a visible-light-excited fluorescent calcium indicator, in conjunction with PE- and PerCP-conjugated MoAbs excited first by a blue 488-nm-line argon ion laser; the APC-conjugated MoAb is then excited by a red 647-nm-line krypton ion laser. An example of a four-color flow cytometry analysis of normal mouse LN cells loaded with fluo-3 and labelled with CD4-PE, CD8-PerCP, and Thy-1.2-APC MoAbs is illustrated in Figure 1. Up to 200,000 cells were recorded during this time course. The triple immunophenotype is displayed in Figure 1A–C. Changes in fluo-3 over time of the whole cell population activated with 12.5 μg/ml ConA (at t = 80 s) is displayed in Figure 1D. The gates R1–R4, which were drawn on the basis of controls for the immunofluorescence described in Materials and Methods, were used throughout this study to analyze simultaneously these changes in each $CD4^+Thy\text{-}1^+$, $CD4^+Thy\text{-}1^-$, and $CD8^+Thy\text{-}1^+$ T-cell subsets and in triple-negative $CD4^-CD8^-Thy\text{-}1^-$ non-T cells. Subsequently, we demonstrated that more than 95% of these non-T cells were $CD45R/B220^+$ (Fig. 5B) when the analysis was gated on lymphocytes on the basis of forward and side scatters. Therefore, they will be considered as B cells in this report.

The general phenotypic pattern obtained here (Fig. 1) was similar to that already described with conventional

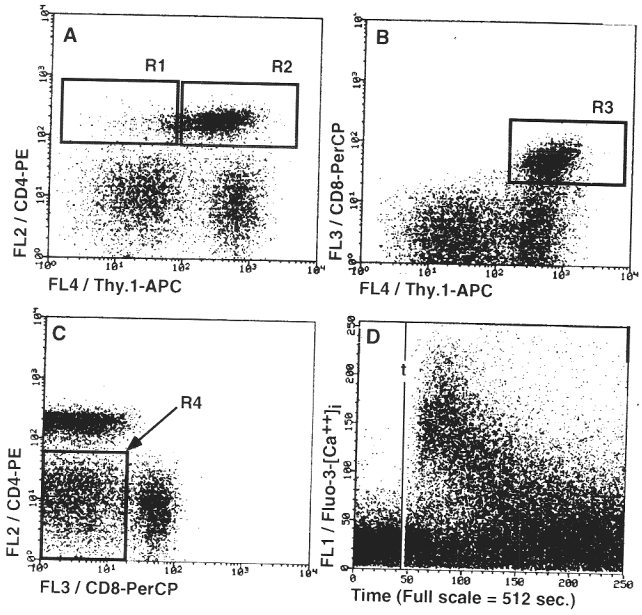

FIG. 1. Four-color flow cytometry of healthy mouse lymph node (LN) cells loaded simultaneously with fluo-3 and labelled with CD4-R-phycoerythrin (PE), CD8-peridinin chlorophyll-α protein (PerCP), and Thy-1.2-allophycocyanin (APC) monoclonal antibodies (MoAbs). **A:** Dot plot of Thy-1.2-APC vs. CD4-PE fluorescences. **B:** Dot plot of Thy-1.2-APC vs. CD8-PerCP fluorescences. **C:** Dot plot of CD8-PerCP vs. CD4-PE fluorescences. **D:** Changes in fluo-3 fluorescence with time of the ungated population activated during the flow cytometry analysis (at time t = 85 s) with 12.5 μg/ml concanavalin A (ConA). A,C: The gates R1–4 were used for on-line simultaneous analysis of these changes in each of the following lymphocytes subsets: R1, $CD4^+Thy\text{-}1^-$ T cells; R2, $CD4^+Thy\text{-}1^+$ T cells; R3, $CD8^+$ T cells; R4, $Thy\text{-}1^-CD4^-CD8^-$ triple-negative non-T cells (most B cells; see Fig. 5). Controls for immunofluorescence are described in Materials and Methods.

one-laser, dual-color flow cytometry using FITC- and PE-conjugated MoAbs (14,38). Accurate analysis was achieved with deliberately suboptimal detection of the red fluorescence emission of APC at 670 nm (DF 670/14 band pass filter) and not at the more optimal 660 nm region, because the standard 660/20 DF filter, as indicated by its 20 nm pass band, did not block the scattered 647 nm excitation laser light. The blue argon laser beam was set deliberately at the lowest possible power of 25 mW in order to avoid the photobleaching of the PerCP molecules (Fig. 2; 48). Specifically, we decreased the power beam four- to tenfold below that generally used with a flow-in-air cytometer. In addition, the voltage or gain of all the photomultiplier tubes (PMTs) and/or of the photodiode was increased consequently to ensure the optimal detection of all signals. Particularly, similar red APC and PerCP fluorescence emissions were separated spatially by the dual-laser stations and were well discriminated by time-delayed fluorescence signals. Spectral overlaps occurred only with the induced fluorescence of the first laser, and conventional electronic compensations between fluo-3 and PE and with PE over PerCP, but not with PerCP over PE, were used. It should be noted

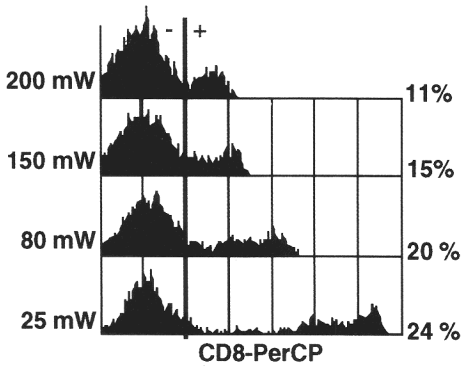

FIG. 2. PerCP photobleaching. An aliquot of cells was labeled with biotinylated CD8 MoAb revealed with PerCP-streptavidin. The cells were analyzed with the FACStar$^+$ flow cytometer in the range of 25–200 mW of laser power. It is demonstrated clearly that the CD8-PerCP high- and low-positive cells were only discriminated at the lowest laser power (25 mW). By increasing the laser power, $CD8^{low}$ cells and a major portion of $CD8^{high}$ cells were lost from the data, as indicated by the decrease in percentage of positively detected cells and by the shift to lower fluorescence channels of the positive part of the histogram.

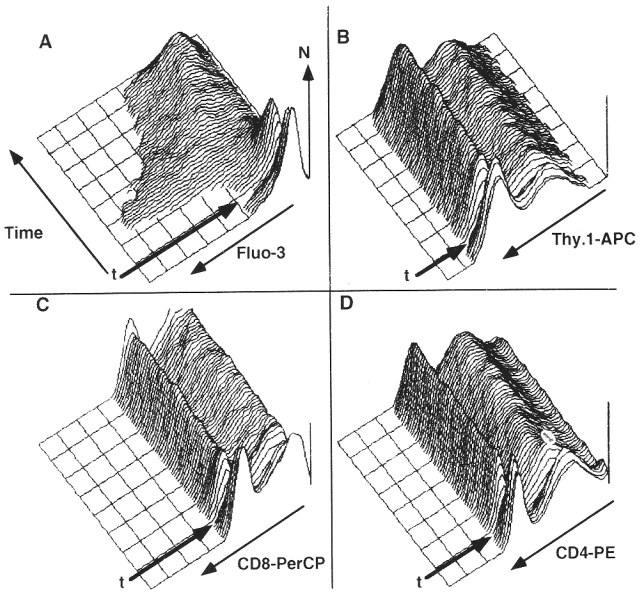

FIG. 3. Simultaneous evolution with time of the fluo-3 signal and of the three-color immunofluorescence distributions of the whole ungated LN lymphocyte populations. The great increase of the fluo-3 signal following the stimulation assay (**A**; ConA; 12.5 μg/ml at time t) affected neither the percentage of positive cells nor the fluorescence distribution of the simultaneously analyzed cell surface markers, Thy-1-APC (**B**), CD8-PerCP (**C**), and CD4-PE (**D**), whose pattern remained unchanged throughout the time course.

that, with the very bright modulated signal of fluo-3, there may be a problem with ensuring constant optimal compensations during the time course when fluo-3 is used at doses higher than 2 μM: a solution to optimize the spectral overlaps is to modulate the compensations during the time course (data not shown). However, under our experimental conditions, an increase of the fluo-3 signal following the stimulation assay affected neither the percentage of positive cells nor the fluorescence intensity distribution of the three cell-surface markers that were maintained constant throughout the time course (Fig. 3), as previously obtained by dual-color flow cytometry (47).

Multiparametric flow cytometric analysis of calcium fluxes in cells gated by their immunofluorescence characteristics have been described previously (28,43). These authors used the UV light calcium probe indo-1 and FITC- and PE-conjugated MoAbs analyzed with a dual UV/blue laser station. Recently, a six-color flow cytometry of calcium response was described in human peripheral blood lymphocytes by using indo-1 (two-color violet/blue ratio) and FITC-, PE-, Texas red-, and APC-conjugated MoAbs (39). However, in these powerful experiments, two colors were used for ratiometric quantitation of calcium ions with indo-1, and three lasers were necessary to allow the determination of $[Ca^{2+}]_i$ in complex immunophenotypic subsets, including a UV laser, a blue argon laser, and a red helium-neon laser.

Fluo-3 extends the potential application field of flow cytometers with visible light lasers to calcium studies of lymphocytes (54). Because the emission characteristics of fluo-3 are virtually identical to those of FITC (25,34), fluo-3 can be combined with almost all of the dyes normally used with multicolor analysis with FITC (42,46, 54). In the domain of calcium measurements that use immunolabelled lymphocyte subsets, this analysis has never been described with more than one immunofluorescence. Fluo-3 was measured generally in two-color flow cytometry with the simultaneous analysis of single cell-surface immunofluorescence performed either with PE-labelled (31,47), or with PE-Texas red tandem-labelled (6), or with PerCP-labelled (13) MoAbs. A more precise ratiometric evaluation of $[Ca^{2+}]_i$ similar to that obtained with indo-1 was described. By combining fluo-3 and the visible light-excited calcium probe fura-red, which exhibits decreased fluorescence intensity upon calcium binding, ratiometrically determined Ca^{2+} fluxes were obtained. Three-color flow cytometry of fluo-3, fura-red, and PE-conjugated MoAb, therefore, can be used to measure $[Ca^{2+}]_i$ accurately in one-color immunolabelled cell subsets (41,42).

Our results (Figs. 1, 3) demonstrate the practical use of fluo-3 in combination with PE-, PerCP-, and APC-labelled MoAbs. This method was improved, as described below, by analysis of calcium flux among resting or stimulated LN lymphocyte subsets from normal mice.

In Situ Four-Color Flow Cytometric Calibration of Fluo-3 Fluorescence

The fluorescence signal recorded from loaded cells reflects not only $[Ca^{2+}]_i$ but also many other factors involving the effective affinity of the calcium dye for Ca^{2+} within the cells at a given pH, ionic strength, free Mg^{2+} concentration, the real concentration of fluo-3 within the cells, and the configuration of the flow cytometer (fil-

ters, photomultipliers tubes, optical pathway) along with less obvious factors, including viscosity, protein concentration, presence of other ions, and photobleaching of the dye (5,12,36,50,52). To avoid these uncertainties, a four-color flow cytometric calibration of fluo-3 signal was made at the end of each experiment with triple-immunolabelled and fluo-3-loaded cells that were incubated with A23187 calcium ionophore and metabolic poisons in a series of graded Ca^{2+}/EGTA buffers with known free Ca^{2+} content. Chused et al. (5) have previously shown that, if cells are first "poisoned" by exposure to metabolic poisons (see Materials and Methods), then the normal membrane gradients collapse, resulting in equal extracellular ($[Ca^{2+}]_o$) and intracellular ($[Ca^{2+}]_i$) calcium concentrations after calcium ionophore treatment. A typical logistic curve was obtained with graded Ca^{2+}/EGTA buffers whose free calcium concentration ranged from 0 to 39.8 μM (Fig. 4). The fluo-3 fluorescence of intact cells gated on the basis of their immunophenotype (Fig. 1) was then a function of the known free calcium concentration of the Ca^{2+}/EGTA buffer and was not cell-subset dependent (Fig. 4B,C). The highest Ca^{2+} concentration (39.8 μM) was enough to saturate the fluo-3 dye, and an apparent maximal fluorescence (F_{max}) was obtained. This Ca^{2+} free concentration is also high enough to saturate the available Ca^{2+} indicators fura-2, indo-1, calcium green, calcium orange, and calcium crimson (36). F_{max} was statistically the same in all subsets (n = 4 experiments). In particular, mean fluo-3 fluorescence differences were not significant between cell subsets at low levels of Ca^{2+} (50–200 nM). An apparent minimal fluorescence (F_{min}) was obtained with the zero calcium free buffer.

By plotting the data of Figure 4B as a double-logarithmic plot (see Fig. 4C), the calculated apparent fluo-3 dissociation constant (K_d) for binding Ca^{2+} (36) was 447 nM at 37°C. This agrees with the original description of fluo-3, which quotes a K_d of 400 nM for binding Ca^{2+} at 22°C (34). However, the binding of fluo-3 to Ca^{2+} is temperature dependant, and a fluo-3 K_d value of 864 nM has been reported by spectrofluorometry of neutrophils and platelets at 37°C (32). The reason for this discrepancy is not clear. However, the effective K_d is definitely sensitive to temperature in addition to ionic strength, free Mg^{2+}, and pH value (12,52). Therefore, it is necessary to determine the true K_d value in each experimental system. In our system, the cells were fluo-3 loaded at room temperature, incubated in 37°C, then analyzed in a flow cytometer with an uncontrolled flow-chamber temperature. Consequently, the mean temperature was below 37°C, and the apparent K_d was 447 nM, which is in the range of 400–860 nM. Finally, the K_d values of 400–450 nM were used by most authors working with fluo-3 at 37°C (6,13,47,54).

A more commonly used, simple flow cytometric method to measure the level of free calcium in intact cells is to calibrate the fluorescence intensity scale for the calcium probe by transporting in saturating Ca^{2+} with calcium ionophore to obtain a maximal signal (F_{max})

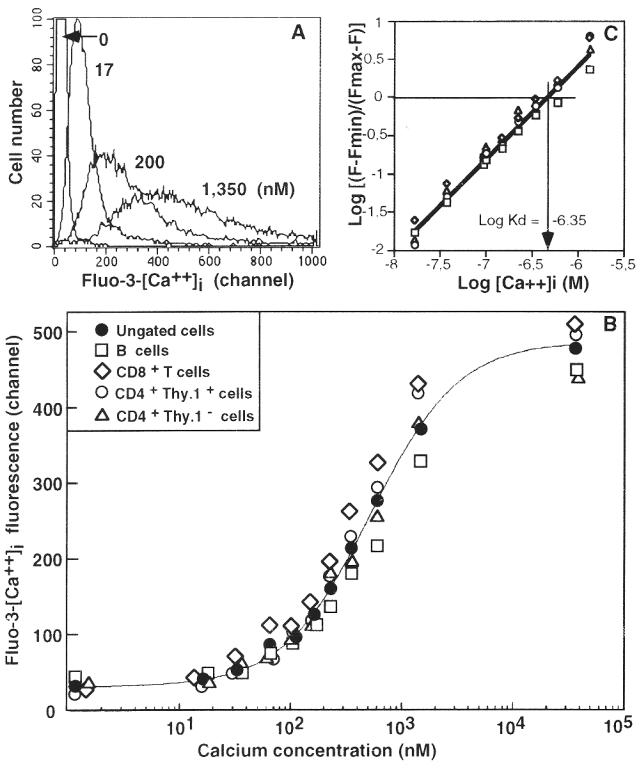

FIG. 4. Calibration of fluo-3. **A:** Distribution of fluo-3 fluorescence of resting LN cells exposed for 2 h at 37°C to a mixture of the metabolic poisons negericin, carbonyl cyanide m-chlorophenylhydrazone (CCCP), and ionophore A23187 in graded Ca^{2+}/EGTA buffers with 100 mM KCl, 10 mM MOPS, pH 7.2. Eleven buffers were used, ranging from 0 to 39.8 μM free Ca^{2+}; only four buffers were selected for the clarity of the figure. The mean fluorescence intensity increased as a function of free Ca^{2+} molarity. **B:** Four-color calibration of fluo-3 in intact cells. The mean fluo-3 fluorescence channel of "poisoned" cells incubated in graded Ca^{2+}/EGTA buffers (A) was measured in the whole LN lymphocyte population (solid circles) and in cell subsets (open symbols) detected with triple immunofluorescence and gated as defined (Fig. 1). There was no statistical differences between cell subsets (t tests; n = 4 experiments). A typical sigmoid curve is fitted (r^2 = 0.998) to mean fluo-3 fluorescence of ungated cells (data from A). **C:** Four-color calibration of fluo-3 derived from B as a double log plot of the molar calcium concentration vs. the ratio $(F - F_{min})/(F_{max} - F)$. F_{min}, F_{max}, and F, respectively, were the mean fluo-3 channel of cells incubated in zero free calcium, in 39.8 μM Ca^{2+}, and in nine intermediate free calcium concentrations. The x-intercept at null ratio (−6.35) is equal to the apparent log K_d indicator (36) and corresponds to an apparent fluo-3-$[Ca^{2+}]$ K_d of 447 nM. Regression line, y = 1.202× + 7.667; r^2 = 0.993.

and then adding $MnCl_2$ to obtain a minimum signal (F_{min}), as was described first for quin-2 (12) and then for fluo-3 (54). The calibration equation for a dye using fluorescence intensity values at one wavelength is then:

$$[Ca^{2+}]_i = K_d (F - F_{min})/(F_{max} - F) \quad (1)$$

(15,25,50,52), where $[Ca^{2+}]_i$ is intracellular ionized calcium concentration, K_d is the dye-dissociation constant for binding Ca^{2+}, and F is the fluorescence of any unknown Ca^{2+} concentration. The applicability of this equation depends on the assumption that fluo-3 binds

Table 1
Calculated Free Calcium Concentrations ($[Ca^{2+}]_i$) in Resting Normal Lymph Node Cells Loaded With Fluo-3 and Labelled Simultaneously With CD4-PE, CD8-PerCP, and Thy-1.2-APC Monoclonal Antibodies Then Analyzed by Four-Color Flow Cytometry[a]

	T cells			B cells
All cells	$CD4^+Thy\text{-}1^-$	$CD4^+Thy\text{-}1^+$	$CD8^+Thy\text{-}1^+$	$CD4^-8^-Thy\text{-}1^-$
103 ± 23	96 ± 13	100 ± 8	80 ± 12**	135 ± 16*

[a]The fluo-3 mean fluorescence base line of unstimulated fluo-3-loaded cells, which were gated as indicated by their immunophenotype, was converted into absolute $[Ca^{2+}]_i$ values by using a direct calibration of fluo-3 fluorescence (Fig. 4). Results are expressed as the mean nanomolar concentration (± standard deviation) of free calcium per cell. PE, R-phycoerythrin; PerCP, peridinin chlorophyll-α protein; APC allophycocyanin.

*Very significantly higher value in B cells compared to each T-cell subset value ($P < 0.001$).

**Lower value in $CD8^+$ T cells with respect to all $CD4^+$ T or B cells ($P < 0.05$; ANOVA, then Newman-Keuls tests; n = 12; four experiments and three mice/group; 50,000 total cells/sample).

Ca^{2+} with stoichiometry 1:1. The slope of the plot in Figure 4C is around 1.0 (1.12 ± 0.15), which reflects this 1:1 binding of each dye molecule with a single Ca^{2+} ion (36).

However, Equation 1 depends also on the assumption that the dye behaves in intact cells as it does in calibration media used in spectrofluorometric measurements with lysed cells. Such a calibration method using intact cells does not compensate for dye loss due to bleaching or leakage during the main recording period. Therefore, the F_{max} value is not accurate, because its value is based on results from intact cells exposed to ionophore without metabolic poisons: The cells defend their intracellular calcium concentration to various degrees, causing a gradient between intra- and extracellular calcium after ionophore treatment.

To verify that the dose of Ca^{2+} ionophore is sufficient to increase $[Ca^{2+}]_i$ to F_{max}, the in situ calibration has to be checked with the lysis method (52). However, in some cell types, such as the insulinoma cell line RINm5F, it is not possible to reach a true F_{max} value, because ionophore treatment does not approach F_{max}, as measured by lysis, unless the ionophore concentration is high enough to cause lysis by itself (52). In addition, F_{min} is determined by adding Mn^{2+}, which quenches all dye fluorescence, leaving only autofluorescence. This is true with quin-2 or fura-2, whereas, with fluo-3, the Mn^{2+}-bound dye has an intermediate fluorescence, making this approach more complicated (15,50). Unfortunately, it has been reported that this method does not work for fluo-3 with lysed cells (50).

Finally, the F, F_{max}, F_{min}, and K_d values must be determined at the same instrumental sensitivity, optical path length, and effective total concentration of dye. These requirements are hard to satisfy when observing cells in a flow cytometer and particularly with a modular, daily-variable, jet-in-air cell sorter. They can be met strictly only in a spectrofluorimeter (12,43).

For all of these reasons, it appears that the use of Equation 1 in flow cytometric experiments is very hazardous unless careful determination of effective K_d, F_{max}, and F_{min} values are performed with the correct temperature and ionic background for each system. Calibration by the use of carefully prepared buffers of known Ca^{2+} content and permeabilization of cells with ionophore and metabolic poisons (5) constitute the most attractive alternative for the accurate determination of absolute calcium concentration in intact cells using a flow cytometer (41).

Absolute Calcium Concentration in Resting Cells

The nanomolar calcium concentration in resting B cells and T-cell subsets was determined by four-color flow cytometry of healthy mouse LN cells loaded simultaneously with fluo-3 and labelled with CD4-PE, CD8-PerCP, and Thy-1.2-APC MoAbs using a direct calibration of fluo-3, as described above. In healthy mice, we obtained mean $[Ca^{2+}]_i$ values per cell in the ranges between 80 ± 12 (15%) and 135 ± 16 nM (12%); [mean ± S.D. (CV%); n = 12 mice], with specific variations among LN lymphocyte subsets (Table 1). The $[Ca^{2+}]_i$ of B cells was clearly higher ($P < 0.001$) with regard to the $[Ca^{2+}]_i$ value of each other T-cell subset.

The reported $[Ca^{2+}]_i$ values in resting T lymphocytes were 107 ± 18 nM (17%) with fluo-3 (54) and, in T-cell lines, in the range between 72 and 136 nM with quin-2 (15,28,53) and between 130–180 nM with indo-1 (43). A value of 100 nM was also reported in splenic mouse lymphocytes with indo-1 (5). Our data are in concordance with the literature. Absolute values, therefore, should be interpreted with some caution, because the true K_d value and other experimental parameters (for example, the slow time-dependent decline in cellular dye content; 54) may be changed during the time-course experiment. However, based on the relative comparisons resulting from a direct calibrated fluo-3 curve without reference to any formula, our conclusions remain unchanged.

Nevertheless, some objections can be raised against the

calcium concentration difference observed between B and T cells. B cells, because they are large cells, are loaded with more fluo-3 than small cells, such as most T cells. The resulting cell-size-dependent fluorescence signal was not corrected for in most fluo-3 experiments. Under some conditions, fluo-3 may be incompletely hydrolyzed and may become compartmentalized within organelles. To minimize this problem, we used Pluronic F-127 and loaded the cells at room temperature, as suggested by Sei and Arora (47). The flow cytometric analysis, however, should be performed at 37°C (or slightly above), because mitogenic stimulation of lymphocytes is a physiological process.

Because the differences we observed between the base-levels of resting cell subsets identified in a four-color experiment (Table 1) could be the result of the naked status of the B cells and of the antibodies bearing T cells, a reciprocal labeling strategy was used (Fig. 5). To measure the calcium base level in naked B and T cells, these subsets were identified with negative selection by staining only one of these cell types with B220-PE MoAb (B cells) and a mixture of CD4-PE and CD8-PE (T cells) MoAbs. Results clearly show that the presence or absence of MoAbs at the cell surface did not affect the measured fluo-3 base levels. Naked B cells (Fig. 5A) or B220-labeled B cells (Fig. 5B) exhibited the same highest calcium base level. The base level of the CD4 cells is higher than in CD8 T cells. This difference was observed using the positive (Fig. 5A) or the negative (Fig. 5B) selection of the T-cell subsets and had the same amplitude in the two conditions. Therefore, this reciprocal observation is not an artifact resulting from fluorescence compensations but reflects a true difference between the calcium base levels of resting B cells and all T-cell subsets that was not due to membrane cross linking. Further experiments are needed to clarify this problem: A means to cancel cell size variation would be to use ratioing between fluo-3 and fura-red signals, as has been described (41,42).

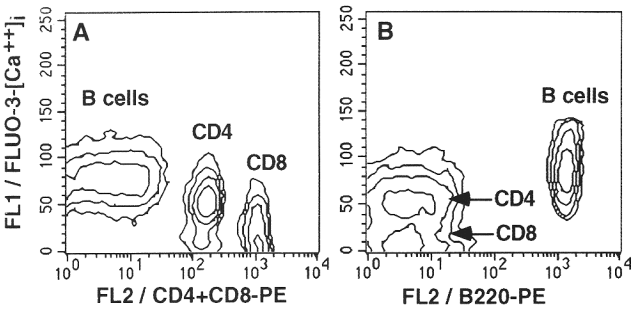

FIG. 5. Dual-color analysis of fluo-3-$[Ca^{2+}]_i$ base-level and reciprocal PE-immunolabeling of T and B resting cells. **A:** The two major T-cell subsets were positively detected with a mixture of CD4-PE MoAb and biotinylated CD8 MoAb revealed with streptavidin-PE molecules and on the basis of a one-log decade difference observed between the PE-fluorescence intensity of $CD4^+$ and $CD8^+$ T cells. The base-line fluo-3 signal is different in all cell subsets and is higher in negatively detected B cells than in positively detected T cells. The base line is also higher in $CD4^+$ T cells than in $CD8^+$ T cells. **B:** Non-T cells were positively detected with B220-PE MoAb, which is a B-cell marker. The base-line fluo-3 signal is different in all cell subsets and is higher in positively detected B cells than in CD4 or CD8 negatively detected T cells. The base-level of $CD4^+$ T cell is higher than in $CD8^+$ T cells. These two T-cell populations are overlapped in the negative cloud, but they were identified as indicated by subsequent analysis after cell sorting experiments (not shown).

Ca^{2+} Response to A23187 Ionophore Is Different in B Cells and T-Cell Subsets

The time course for calcium mobilization was analyzed with the four-color technique simultaneously among B cells and $CD8^+$, $CD4^+Thy\text{-}1^+$, and $CD4^+Thy\text{-}1^-$ T-cell subsets after in vitro stimulation with A23187 calcium ionophore. Figure 6 shows that the calcium response of A23187 ionophore-stimulated lymphocytes was heterogeneous among the cell subsets. Both the intensity and the shape of the fluo-3 signal response plotted against time were different between B cells and T cells and between the CD4 and CD8 T-cell subsets. The fluo-3 in the B cells reached the highest fluorescence intensity about 3.5 min after the ionophore-stimulation time; the fluorescence level slowly decreased afterward, to reach the base line about 6.6 min after the beginning of the stimulation time. This bell-shaped curvature of the fluo-3 vs. time function obtained with A23187 stimulation was a reproducible feature of B cells. By contrast, the response of T cells was characterized by a plateau level of fluo-3 fluorescence reached as soon as 1 min after stimulation. This constant level of the T-cell response was maintained up to 8 min, whereas the fluorescence base level of the B cells was already restored. The response of the $CD4^+$ T cells was far more intense than the low response of the $CD8^+$ T cells (Fig. 6B,C). In the $CD4^+$ T-cell population, there was no significant difference whether these cells expressed Thy-1.2 antigen or not (Fig. 6C,D).

A trivial explanation for the difference between T- and B-cell ionophore responses would be differential uptake of the ionophore by the two cell types. However, this hypothesis is certainly not true, because A23187 uptake is not different between the B and T cells in the spleen of BALB/c mice (20). B-cell ^{45}Ca efflux increased in the presence of ionomycin, whereas T-cell efflux did not, leading to a maintained $[Ca^{2+}]_i$ level in T cells but not in B cells. This observation suggests that the B- cell calcium pump is intrinsically more active than the T-cell pump at elevated $[Ca^{2+}]_i$, a phenomenon that is related to the depolarized potential membrane of B cells and the hyperpolarized state of T cells produced by opening K^+ channels (20). The heterogeneity of lymphocyte calcium metabolism is caused by T-cell-specific, calcium-sensitive, potassium channel response to $[Ca^{2+}]_i$ and by the sensitivity of the calcium ATPase pump to membrane potential. Our observation of a short time response of B cells and a long-time sustained response of T cells to A23187 ionophore is in agreement with these views.

The heterogeneity in calcium response to ionophore A23187 between B cells and $CD4^+$ and $CD8^+$ T cells strengthens the impression of profound differences between these cell populations. These differences between

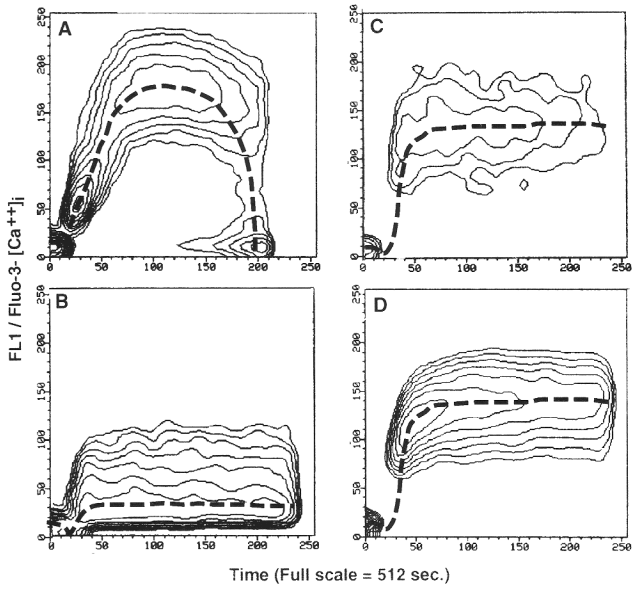

FIG. 6. Heterogeneous responses in fluo-3 over time observed simultaneously in different normal LN lymphocyte subsets after stimulation with the A23187 calcium ionophore (10 μM) at time t = 30 s. **A:** B cells. **B:** $CD8^+$ T cells. **C:** $CD4^+Thy\text{-}1^-$ T cells. **D:** $CD4^+Thy\text{-}1^+$ T cells. The dashed lines illustrate the evolution with time of the mean fluo-3 fluorescence intensity. Contour plots (log scale of cell number), 200,000 total events.

$CD4^+$ and $CD8^+$ T-cell subsets, which are described here for the first time, are due neither to surface antigen expression nor (probably) to protein kinase (PTK) associated to these molecules, because the site of action of A23187 is receptor independent and also may be independent of phosphoinositide hydrolysis. However, it has been shown that mitogenic concentrations of A23187 cause an increase in the net phosphorylation of phosphatidylinositol PI to PI(4,5)P2 in mouse thymocytes (49). Others have shown that, in LN T cells, the proportion of $p56^{Lck}$ (a PTK that is associated physically with CD4 and CD8 molecules and that participates in signal transduction), which is associated with CD4 molecules, is 10- to 20-fold higher than that associated with CD8 molecules (22). This difference may explain not only the response heterogeneity between these subsets to A23187 but also the response to lectins (see below).

The calcium ionophore A23187 was also found to induce a heterogeneous proliferation responsive of the murine $CD4^+$ T-cell subset (24). Interestingly, neither $CD8^+$ T cells nor B cells responded to the calcium ionophore by proliferation (10,24). The inability of $CD8^+$ T cells to proliferate after A23187-ionophore stimulation was probably due to insufficient production of autocrine growth factors (IL2), inasmuch as the addition of exogenous IL-2 completely restores the $CD8^+$ T-cell responsiveness (23). These differences in the proliferative response of T-cell subsets after A23187 stimulation are corroborated by the differences we observed in calcium fluxes among lymphocyte subsets.

Calcium Mobilization Following a Lectin Stimulation Is Time Delayed in $CD4^+$ and $CD8^+$ T Cells, but Not in B Cells

A time course for Ca^{2+} mobilization induced by ConA in B cells and in $CD4^+$ and $CD8^+$ T-cell subsets from LN of a normal mouse is illustrated in Figure 7. The different cell subsets have a different response to the stimulus. The response of B cells to ConA increased rapidly in less than 25 s and reached the highest calcium mobilization level in the first min following the stimulation at time t (Fig. 7A). The response of all T-cell subsets was time delayed by 80 s (Fig. 7B,C); then, an increase of the fluo-3 signal was observed clearly, but with a higher intensity among $CD4^+$ T cells (Fig. 7B) than among $CD8^+$ T cells (Fig. 7C). There was no significant difference between the response of $CD4^+$ T cells lacking or bearing the Thy-1 antigen (data not shown), and their kinetics were identical to the data shown in Figure 7B for the whole $CD4^+$ population. The rapid and strong mobilization of $[Ca^{2+}]_i$ in LN B cells after stimulation with ConA (Fig. 7A) was a systematically reproducible observation, which has been described in spleen cells (2,47). Similarly, we observed a time-delayed response of the T-cell subsets but not of the B cells upon PHA stimulation (Fig. 8). In contrast, calcium mobilization in T cells with anti-CD3 MoAb stimulation was induced rapidly without a detectable time delay (Fig. 9). The reasons for the differential time effects of these stimuli are unknown. However, the fact that a time delay may exist in response to lectin stimuli but not to anti-CD3 MoAb stimulation suggests that a membrane receptor-dependent mechanism is involved rather than a postreceptor effect.

Percentage of Responding Cells Among B- and T-Lymphocyte Subsets on In Vitro Stimulation With Different Mitogens

With the simultaneous use of fluo-3 and three MoAbs against CD4, CD8, and Thy-1 antigens (PE-, PerCP-, and APC-conjugated MoAbs, respectively), it was possible to determine accurately the frequency of cells showing an increased $[Ca^{2+}]_i$ in response to stimulation with ConA, PHA, or anti-CD3 MoAbs among the gated B cells and among the CD8 and CD4 (bearing or lacking the Thy-1 antigen, respectively) T-cell subsets (Table 2).

Comparison of B- and T-cell populations. Both the T- and B-cell subsets showed an increase of fluo-3 fluorescence upon in vitro stimulation with ConA (Fig. 7) or with PHA (Fig. 8), but only the T cells responded to anti-CD3 MoAbs (Fig. 9; Table 2). This is in agreement with other results (2,47). The percentage of responding cells upon stimulation with ConA was higher in T cells than in B cells. In contrast, PHA resulted in a higher response in B cells (Table 2). The reason for this difference is unknown. However, the qualitative difference in lectin-binding antigen between the two subsets may contribute to explaining this heterogeneity: The lectin binds to the TCR/CD3 antigen-receptor complex on human T cells and to IgM and IgD and both class I and class II

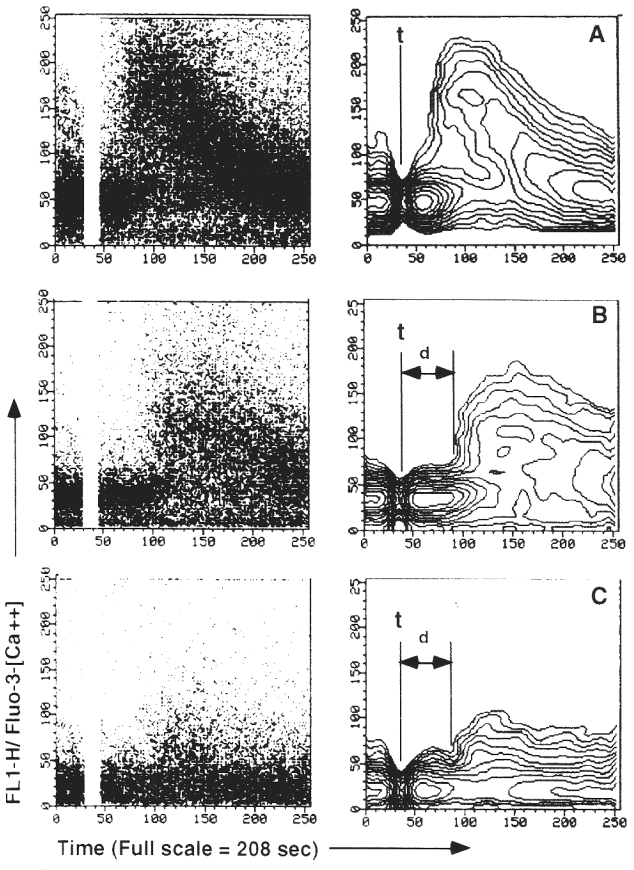

FIG. 7. Changes in fluo-3 fluorescence intensity as a function of time analyzed simultaneously in LN lymphocyte subsets detected with triple immunofluorescence and gated as defined (Fig. 1). The cells were activated at time t = 30 s with 12.5 μg/ml ConA. Each cell subset displays a unique response to the stimulus. A marked time-delay of 80 s (d) was clearly observed in the response of both the $CD4^+$ (B) and the $CD8^+$ (C) T cells. **A:** B cells. **B:** Whole $CD4^+$ T cells. **C:** $CD8^+$ T cells. Left, dot plot (80,000 total events); right: contour plot (log scale of cell number).

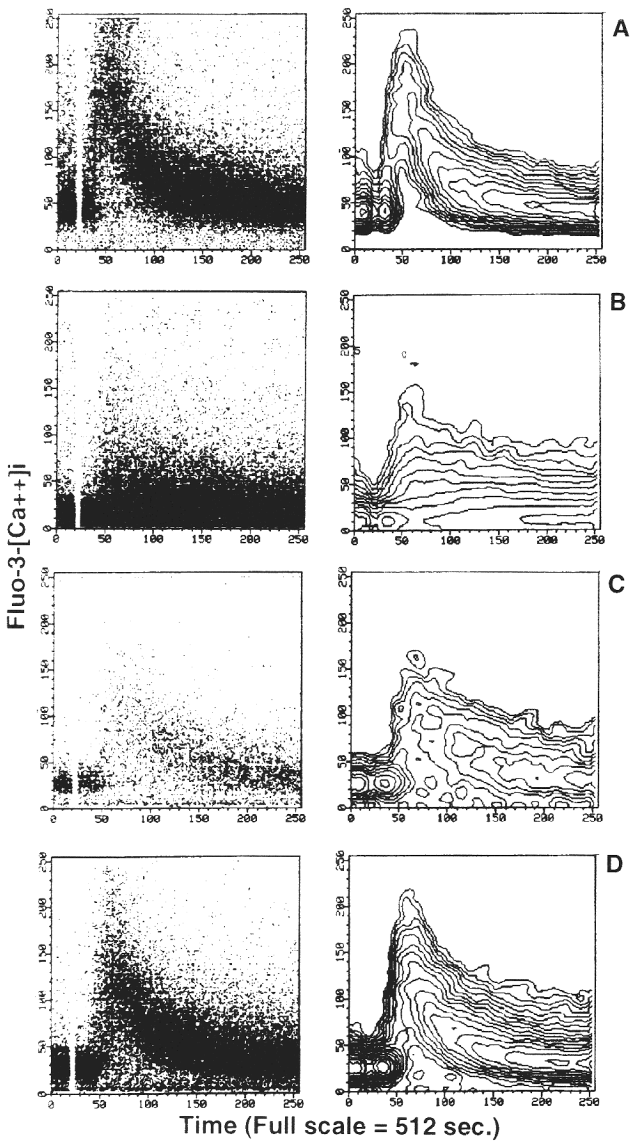

FIG. 8. Changes in fluo-3 fluorescence intensity as a function of time analyzed simultaneously in LN lymphocyte subsets detected with triple immunofluorescence and gated as defined (Fig. 1). The cells were activated at time t = 30 s with 10 μg/ml PHA. Each cell subset displays a unique response to the stimulus. The response of the $CD4^+Thy\text{-}1^+$ T cells was far more robust than the response of the $CD4^+Thy\text{-}1^-$ or the $CD8^+$ T cells (Table 2). **A:** B cells. **B:** $CD8^+$ T cells. **C:** $CD4^+Thy\text{-}1^-$ T cells. **D:** $CD4^+Thy\text{-}1^+$ T cells. Left, dot plot (80,000 total events); right, contour plot (log scale of cell number).

major histocompatibility complex antigens on murine B cells (2).

Comparison of $CD4^+$ and $CD8^+$ T cells. After stimulation with different mitogens, $[Ca^{2+}]_i$ increased in both $CD4^+$ and $CD8^+$ T-cell subsets (Figs. 7–9). However, the percentage of responding cells was highest in the $CD4^+$ subset (Table 2). Our results with PHA or anti-CD3 MoAb are in agreement with other studies on human lymphocytes (43). However, our results conflict with those reported in the mouse spleen by Sei and Arora (47) showing that the $CD8^+$ T cells responded more strongly to ConA than the $CD4^+$ T cells. This discordance is unclear, but these authors used ConA at a concentration of 1 μg/ml, compared to our 12.5 μg/ml. It has been discussed above that, in primary LN T cells, 75–95% of cellular protein tyrosine kinase $p56^{Lck}$ is associated physically with CD4, but only 5–10% is associated with CD8 molecules (22). In other hands, mouse $CD4^+$ splenic T cells (but not $CD8^+$ T cells) increased $[Ca^{2+}]_i$ after CD28 cross linking, indicating a distinct signal transduction in the two subsets after CD28 receptor ligation (1). All of these differences can explain the response heterogeneity between these subsets to the receptor-dependant stimuli and, particularly, the highest response to lectins and anti-CD3 MoAb we observed with mouse $CD4^+$ LN T cells.

Comparison of $CD4^+Thy\text{-}1^+$ and $CD4^+Thy\text{-}1^-$ T cells. Comparison of $CD4^+$ cells bearing or lacking the Thy-1 antigen showed that the percentage of responding cells in the $CD4^+Thy\text{-}1^+$ subset was higher than in the

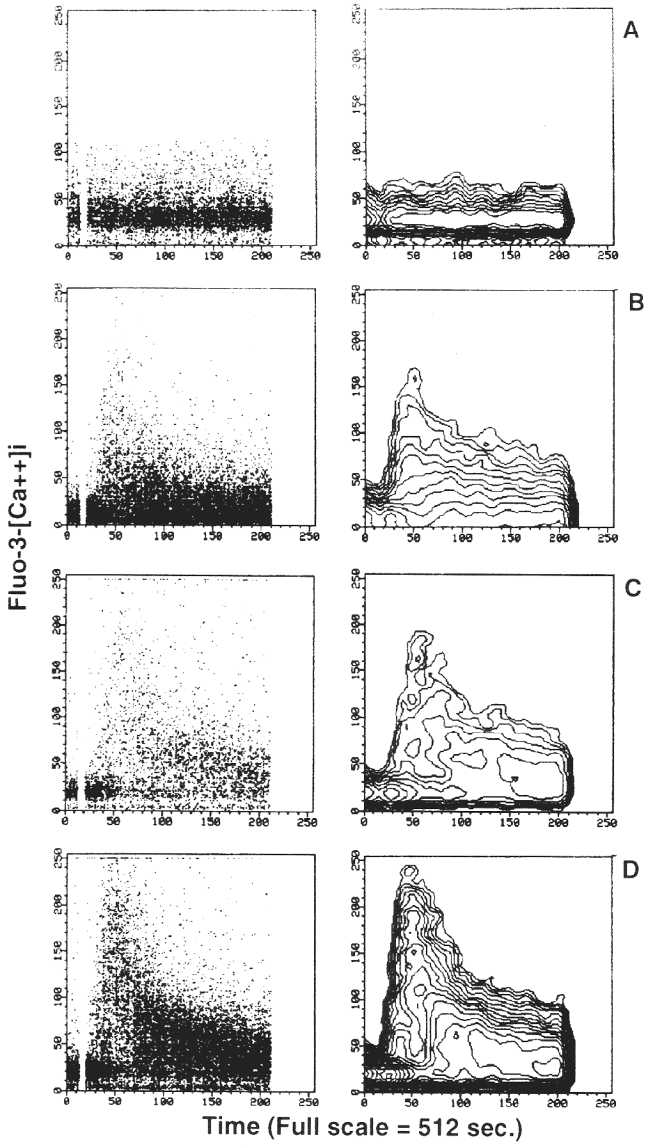

FIG. 9. Changes in fluo-3 fluorescence intensity as a function of time analyzed simultaneously in LN lymphocyte subsets detected with triple immunofluorescence and gated as defined (Fig. 1). The cells were activated at time t = 30 s with 5 μg/ml anti-CD3 MoAb (145-2C11). The response of T cells, but not of B cells, was characterized by an increase of the fluo-3 fluorescence signal. The response of the $CD4^+Thy\text{-}1^+$ T cells was far more robust than the response of the $CD4^+Thy\text{-}1^-$ or the $CD8^+$ T cells (Table 2). **A:** B cells. **B:** $CD8^+$ T cells. **C:** $CD4^+Thy\text{-}1^-$ T cells. **D:** $CD4^+Thy\text{-}1^+$ T cells. Left, dot plot (80,000 total events); right, contour plot (log scale of cell number).

$CD4^+Thy\text{-}1^-$ T-cell subset upon stimulation with ConA, PHA, or anti-CD3 MoAbs (Table 2). Because the Thy-1 molecule is associated with intracytoplasmic protein tyrosine kinase $p59^{fyn}$ (51), this molecule could participate in signal transduction. However, stimulation with unlabelled anti-Thy-1 MoAbs did not induce calcium mobilization in $Thy\text{-}1^+$ lymphocytes (data not shown). It has been demonstrated in humans that antibodies binding to

Table 2
Percentage of Responding B- and T-Cell Subsets From Normal Mouse Lymph Nodes With In Vitro Stimulation With Different Mitogens Using a Single-Tube, Four-Color Assay[a]

Cell subsets	ConA	PHA	Anti-CD3
Lymph node cells			
B	33.5 ± 6.0	42.7 ± 10.9	0.0
T (all)*	47.7 ± 13.0	23.5 ± 8.9	52.8 ± 5.5
T cells			
CD8**	27.5 ± 9.9	16.2 ± 2.6****	45.0 ± 7.0****
CD4 (all)**	43.0 ± 12.4	31.7 ± 9.1	61.6 ± 2.8
$Thy\text{-}1^-$***	42.5 ± 12.5	19.5 ± 6.7****	46.0 ± 8.6****
$Thy\text{-}1^+$***	53.3 ± 13.6	30.4 ± 9.9	64.0 ± 3.6

[a]Numbers indicate the percentages (mean ± S.D.; n = 20 mice) of responding cells showing increased $[Ca^{2+}]_i$ (increased fluo-3 fluorescence intensity) detected at maximal calcium mobilization following a stimulation with either concanavalin A (ConA; 12.5 μg/ml), phytohaemagglutinin (PHA; 10 μg/ml), or anti-CD3 monoclonal antibodies (MoAbs; 5 μg/ml; clone 145-2C11). Measurements were performed by using single-tube, four-color assays labelled simultaneously with fluo-3, CD4-PE, CD8-PerCP, and Thy-1.2-APC MoAbs. Background was deduced, defined as the percentage of fluo-3-positive cells detected before the stimulation above 95% of maximal fluo-3 intensity determined at baseline.

*Significant difference ($P < 0.05$) between the whole T-cell population and the B cells for the three conditions.

**Significant difference ($P < 0.05$) between the whole CD4 T-cell population and the CD8 T cells for the three conditions.

***Very significant difference ($P < 0.01$) between the $CD4^+Thy\text{-}1^+$ and the $CD4^+Thy1^-$ T-cell subsets for the three conditions.

****No significant difference between the $CD4^+Thy\text{-}1^-$ and the CD8 T-cell subsets stimulated either with PHA or anti-CD3 MoAbs (ANOVA, then Newman-Keuls tests).

a large subset of T-cell differentiation antigens, including CD2, CD4, CD5, CD6, CD7, CD8, Tp44, and CDw18, cause an increase in the cytoplasmic calcium concentration after the antigens are cross linked on the cell surface (28). In the mouse, prior to cross linking with a second-step antibody, none of the anti-Thy-1, anti-CD4 (L3T4), or anti-CD8 (Lyt-2) MoAbs caused a change in $[Ca^{2+}]_i$, except for anti-CD3 (28). In the present study, we exclusively used direct fluorochrome-conjugated primary antibodies that did not induce a detectable variation in the $[Ca^{2+}]_i$ of resting cells (data not shown). Therefore, the binding of anti-Thy-1 MoAbs to the surface of Thy-1-bearing T cells could not explain the higher calcium response of the $CD4^+Thy\text{-}1^+$ T cells with respect to their $Thy\text{-}1^-$ counterparts.

Therefore, the signal provided by the Thy-1 molecule seems to be important, but it is insufficient for calcium mobilization and T-cell activation. Interestingly, the calcium response of the minor $CD4^+Thy\text{-}1^-$ T-cell subpopulation (<4% of the whole cell population) was similar to the cell response of the $CD8^+$ T cells with PHA stimulation (20% of responding cells) or with anti-CD3 MoAb stimulation (45% of responding cells), but it showed a higher response to ConA stimulation (Table 2).

In conclusion, this work demonstrates the practical feasibility of using fluo-3 simultaneously with up to three

FITC-compatible fluorochromes. This method offers the opportunity to analyze, in one step in the same sample, the calcium flux in complex immunophenotypic subsets with visible excitation-light flow cytometers.

ACKNOWLEDGMENTS

We thank the Foundation for Scientific Medical Research (FRSM), Télévie, and the Faculty of Medicine of Liège University for supporting this research. M.M. is a Senior Research Assistant of the National Fund for Scientific Research (Belgium, FNRS). The authors thank Mrs. E. Franzen-Detrooz for her expert technical assistance.

LITERATURE CITED

1. Abe R, Vandenberghe P, Craighead N, Smoot DS, Lee KP, June CH: Distinct signal transduction in mouse $CD4^+$ and $CD8^+$ splenic T cells after CD28 receptor ligation. J Immunol 154:985–997, 1995.
2. Bijsterbosch MK, Klauss GGB: Concanavalin A induces Ca^{2+} mobilization, but only minimal inositol phospholipid breakdown in mouse B cells. J Immunol 137:1294–1299, 1986.
3. Cerny A, Hügin AW, Holmes K, Morse HC III: $CD4^+$ T cells in murine acquired immunodeficiency syndrome: Evidence for an intrinsic defect in the proliferative response to soluble antigens. Eur J Immunol 20:1577–1581, 1990.
4. Colombi S, de Leval L, Deprez M, Humblet C, Greimers R, Defresne MP, Boniver J, Moutschen M: Thymus involvement in murine acquired immunodeficiency (MAIDS). Thymus 23:27–37, 1994.
5. Chused TM, Wilson HA, Greenblatt D, Ishida Y, Edison LJ, Tsien RY, Finkelman FD: Flow cytometric analysis of murine splenic B lymphocyte cytosolic free calcium response to anti-IgM and anti-IgD. Cytometry 8:396–404, 1987.
6. De Maria R, Fais S, Silvestri M, Frati L, Pallone F, Santoni A, Testi R: Continuous in vivo activation and transient hyporesponsiveness to TcR/CD3 triggering of human gut lamina propria lymphocytes. Eur J Immunol 23:3104–3108, 1993.
7. Donnadieu E, Bismuth G, Trautmann A: Calcium fluxes in T lymphocytes. J Biol Chem 267:25864–25872, 1992.
8. Donnadieu E, Bismuth G, Trautmann A: Antigen recognition by helper T cells elicits a sequence of distinct changes of their shape and intracellular calcium. Curr Biol 4:584–595, 1994.
9. Fitzpatrick EA, Bryson JS, Rhoads C, Kaplan AM, Cohen DA: T-deficient transmembrane signaling in $CD4^+$ T cells of retroviral-induced immune-deficient mice. J Immunol 148:3377–3384, 1992.
10. Freedman MH, Khan MR, Trew-Marshall BJ, Cupples CG, Mely-Gaubert B: Early biochemical events in lymphocytes activation. II. Selectivity of A23187 for T lymphocytes and the use of an apolar fluorescent probe (1,6-diphenyl-1,3,5-hexatriene) to monitor ionophore- and lectin-induced lymphocytes activation. Cell Immunol 58: 134–146, 1981.
11. Gardner P: Calcium and T lymphocyte activation. Cell 59:15–19, 1989.
12. Grynkiewicz G, Poenie M, Tsien RY: A new generation of Ca^{2+} indicators with greatly improved fluorescence properties. J Biol Chem 260:3440–3450, 1985
13. Guillaume T, Hamdan O, Staquet P, Sekhavat M, Chatelain B, Bosly A, Rubinstein DB, Humblet Y, Doyen C, Coiffier B: Blunted rise in intracellular calcium in $CD4^+$ T cells in response to mitogen following autologous bone marrow transplantation. Br J Haematol 84: 131–136, 1993.
14. Harriman GR, Lycke NY, Elwood LJ, Strober W: T lymphocytes that express CD4 and the αβ-T cell receptor but lack Thy-1. Preferential localization in Peyer's patches. J Immunol 145:2406–2014, 1990.
15. Hesketh TR, Smith GA, Moore JP, Taylor MV, Metcalfe JC: Free cytoplasmic calcium concentration and the mitogenic stimulation of lymphocytes. J Biol Chem 258:4876–4882, 1983.
16. Hiromatsu K, Aoki Y, Makino M, Matsumoo Y, Mizuochi T, Gotoh Y, Nomoto K, Ogasawara J, Nagata S, Yoshikai Y: Increased Fas antigen expression in murine retrovirus-induced immunodeficiency syndrome, MAIDS. Eur J Immunol 24:2446–2451, 1994.
17. Holmes KL, Morse HC III, Makino M, Hardy RR, Hayakawa K: A unique subset of normal murine $CD4^+$ T cells lacking Thy-1 is expanded in a murine retrovirus-induced immunodeficiency syndrome, MAIDS. Eur J Immunol 20:2783–2787, 1990.
18. Isakov N, Mally MI, Scholz W, Altman A: T-lymphocyte activation: The role of protein kinase C and the bifurcating inositol phospholipid signal transduction pathway. Immunol Rev 95:89–111, 1987.
19. Iseki R, Mukai M, Iwata M: Regulation of T lymphocyte apoptosis. Signals for the antagonism between activation- and glucocorticoid-induced death. J Immunol 147:4286–4292, 1991.
20. Ishida Y, Chused TM: Heterogeneity of lymphocyte calcium metabolism is caused by T cell-specific calcium-sensitive potassium channel and sensitivity of the calcium ATPase pump to membrane potential. J Exp Med 168:839–852, 1988.
21. Jolicoeur P: Murine acquired immunodeficiency syndrome (MAIDS): An animal model to study the AIDS pathogenesis. FASEB J 5:2398–2405, 1991.
22. Julius M, Maroun CR, Haughn L: Distinct roles for CD4 and CD8 as co-receptors in antigen receptor signalling. Immunol Today 14(4): 177–183, 1993.
23. June CH, Rabinovitch PS: Flow cytometric measurement of intracellular ionized calcium in single cells with indo-1 and fluo-3. In: Methods in Cell Biology, Vol 33: Flow Cytometry, Darzynkiewicz Z, Crissman HA (eds). Academic Press, London, 1990, pp 37–58.
24. Kakkanaiah VN, Nagarkatti PS, Nagarkatti M: Murine lymphocytes exhibit heterogeneity in their proliferative responsiveness to calcium ionophore. Cell Mol Biol 38:533–543, 1992.
25. Kao JPY, Harootunian AT, Tsien RY: Photochemically generated cytosolic calcium pulses and their detection by fluo-3. J Biol Chem 264:8179–8184, 1989.
26. Katayamana Y, Miyazaki S, Oshimi Y, Oshimi K: Ca^{2+} response in single human T cells induced by stimulation of CD4 or CD8 and interference with CD3 stimulation. J Immunol Methods 166:145–153, 1993.
27. Kroczek RA, Gunter KC, Germain RN, Shevach EM: Thy-1 functions as a signal transduction molecule in T lymphocytes and transfected B lymphocytes. Nature 322:181–184, 1986.
28. Ledbetter JA, June CH, Grosmaire LS, Rabinovitch PS: Crosslinking of surface antigens causes mobilization of intracellular ionized calcium in T lymphocytes. Proc Natl Acad Sci USA 84:1384–1388, 1987.
29. Legrand E, Daculsi R, Duplan JF: Characteristics of the cell populations involved in extra-thymic lymphosarcoma induced in C57BL/6 mice by RadLV-Rs. Leukemia Res 5:223–233, 1981.
30. Leo O, FooM, Sachs DH, Samelson LE, Bluestone JA: Identification of a monoclonal antibody specific for a murine T3 polypeptide. Proc Natl Acad Sci USA 84:1374–1378, 1987.
31. Makino M, Sei Y, Arora PK, Morse HC III, Hartley JW: Impaired calcium mobilization in $CD4^+$ and $CD8^+$ T cells in a retrovirus-induced immunodeficiency syndrome, murine AIDS. J Immunol 149: 1707–1713, 1992.
32. Merrit JE, McCarthy A, Davies MPA, Moores KE: Use of fluo-3 to measure cytosolic Ca^{2+} in platelets and neutrophils. Biochem J 269: 513–519, 1990.
33. Miller RA, Philosophe B, Ginis I, Weil G, Jacobson B: Defective control of cytoplasmic calcium concentration in T lymphocytes from old mice. J Cell Physiol 138:175–182, 1989.
34. Minta A, Kao JPY, Tsien RY: Fluorescent indicators to cytosolic calcium based on rhodamine and fluorescein chromophores. J Biol Chem 264:8171–8178, 1989.
35. Mizuochi T, Mizuguchi J, Uchida T, Ohnishi K, Nakanishi M, Asano Y, Kakiuchi T, Fukushima Y, Okuyama K, Morse HC III, Komuro K: A selective signal defect in helper T cells induced by antigen-presenting cells from mice with murine acquired immunodeficiency syndrome. J Immunol 144:313–316, 1990.
36. Molecular Probes, Inc: Calcium calibration buffer kits. Product information sheet MP 3008, Molecular Probes, Eugene, OR, 1995.
37. Mosier DE, Yetter RA, Morse HC III: Retroviral induction of acute lymphoproliferative disease and profound immunosuppression in adult C57/BL6 mice. J Exp Med 161:766–784, 1985.
38. Moutschen MP, Colombi S, Deprez M, Van Wijk F, Hotermans C,

Martin MT, Greimers R, Boniver J: Population dynamics of $CD4^+$ T cells lacking Thy-1 in murine retrovirus-induced immunodeficiency syndrome (MAIDS). Scand J Immunol 39:216–224, 1994.

39. Mylvaganam R, Horton A: Six color flow cytometry of calcium response in human peripheral blood lymphocytes. XVII Congress of the International Society for Analytical Cytology. Cytometry Suppl 7:85A, 1994 (abstract).
40. Nathanson MH, Burgsthaler AD: Coordination of hormone-induced calcium signals in isolated rat hepatocyte couplets: Demonstration with confocal microscopy. Mol Biol Cell 3:113–121, 1992.
41. Novak EJ, Rabinovitch PS: Improved sensitivity in flow cytometric intracellular ionized calcium measurement using fluo-3/fura red fluorescence ratios. Cytometry 17:135–141, 1994.
42. Rabinovitch PS, June CH: Intracellular ionized calcium, magnesium, membrane potential, and pH. In: Flow Cytometry, A Practical Approach, Ed 2, Ormerod MG (ed). IRL Press at Oxford University Press, New York, 1994, pp 185–215.
43. Rabinovitch PS, June CH, Grossmann A, Ledbetter JA: Heterogeneity among T-cells in intracellular free calcium responses after mitogen stimulation with PHA or anti-CD3. Simultaneous use of indo-1 and immunofluorescence with flow cytometry. J Immunol 137:952–961, 1986.
44. Rabinovitch PS, June CH: Measurement of intracellular ionized calcium and membrane potential. In: Flow Cytometry and Sorting, Ed 2, Melamed MR, Lindmo T, Mendelsohn ML (eds). John Wiley and Sons, Inc., New York, 1990, pp 651–668.
45. Rasmussen H: The calcium messenger system. N Engl J Med 314: 1094–1101, 1986.
46. Rijkers GT, Justement LB, Griffionen AW, Cambier JC: Improved method for measuring intracellular Ca^{2+} with fluo-3. Cytometry 11:923–927, 1990.
47. Sei Y, Arora PK: Quantitative analysis of calcium (Ca^{2+}) mobilization after stimulation with mitogens or anti-CD3 antibodies. J Immunol Methods 137:237–244, 1991.
48. Shapiro HM: Practical Flow Cytometry, Ed 3. Wiley-Liss, Inc., New York, 1995.
49. Taylor MV, Metcalfe JC, Hesketh TR, Smith GA, Moore JP: Mitogens increase phosphorylation of phosphoinositides in thymocytes. Nature 312:462–465, 1984.
50. Thomas AP, Delaville F: The use of fluorescent indicators for measurements of cytosolic-free calcium concentration in cell populations and single cells. In: Cellular Calcium: A Practical Approach, McCormack JG, Cobbold PH (eds). IRL Press at Oxford University Press, New York, 1991, pp 1–54.
51. Thomas PM, Samelson LE: The glycophosphatidylinositol-anchored Thy-1 molecule interacts with the $p60^{fyn}$ protein tyrosine kinase in T-cells. J Biol Chem 267:12317–12322, 1992.
52. Tsien R, Pozzan T: Measurement of cytosolic free Ca^{2+} with quin2. Methods Enzymol 172:230–262, 1989.
53. Tsien RY, Pozzan T, Rink TJ: Calcium homeostasis in intact lymphocytes: Cytoplasmic free calcium monitored with a new intracellular trapped fluorescent indicator. J Cell Biol 94:325–334, 1987.
54. Vandenberghe PA, Ceuppens JL: Flow cytometric measurement of cytoplasmic free calcium in human peripheral blood T lymphocytes with fluo-3, a new fluorescent calcium indicator. J Immunol Methods 127:197–205, 1990.